J. Al-Azhar University –Gaza 2004, Vol. 7, NO. 2 P 63-74

A Study of Multi-Nucleon Transfer Reactions Using Yukawa Potential

A.A.Farra[(1)], A.I.Assa'd[(2)]

[(1)] Physics Department, Al–Azhar University, Gaza, Palestine.

[(2)] Physics Department, Al–Aqsa University, Gaza, Palestine.

Received: 13 June 2004 / Accepted: 1 March 2005

Abstract: The differential cross-sections of heavy-ion transfer reactions have been calculated in terms of the distorted wave Born approximation (DWBA) analysis using Woods-Saxon optical model potential. The form factor of the transferred cluster was calculated using the standard separation energy procedure. The calculated angular distributions are found to be in good agreement with the experimental data. The inclusion of the J-dependent absorptive term reproduces quite well the shapes and magnitudes of the cross-section and leads to a better description to the large angle data than the phenomenological Woods-Saxon potential.

Keywords: Incident energy= 20-56 MeV, DWBA, calculated $\sigma(\theta)$.

INTRODUCTION

The quasielastic cross-sections were successfully analyzed within the framework of a simple DWBA calculations using a Woods-Saxon optical model potential at energies of about 40% of the coulomb barrier [1]. At energies below and above the Coulomb barrier, the calculated DWBA cross-sections using spectroscopic amplitudes obtained from shell model calculations were found in agreement with the experimental data of two–nucleon transfer reactions [2,3]. The uprising oscillatory structures of heavy-ion reactions with alpha particle transfer have been clearly described in terms of the nuclear molecular-orbital theory [4,5] where the finite-range DWBA calculations following one- and two step processes introduce a poor description for both angular distributions and excitation functions. In addition, the oscillatory structures of the differential cross-sections at back-ward regions were adequately explained in terms of a deep alpha polarization potential [6], density-dependent calculations [7] and double-folding model [8,9].

In the present work, the differential cross-sections and form factors have been calculated for different reactions which proceed via direct two-or three-nucleon or alpha particle transfer processes using a simple one-step DWBA method. The optical model potential is modified to include a cutoff angular momenta term. The bound state form factors described in term of Yukawa potential with parameters chosen to reproduce the corresponding cluster-nucleus binding energies. In the present study we consider ^{48}Ca(^{16}O,^{14}C)^{50}Ti, ^{64}Ni(^{16}O,^{14}C)^{66}Zn, ^{16}O(^{7}Li,α)^{19}F and ^{24}Mg(^{16}O,^{12}C)^{28}Si reactions.

In section 2, the DWBA formulation for the finite-range form factor is described. Numerical calculations and results are given in section 3. Section 4 is left for discussion and conclusions.

One-Step DWBA Analysis

In the present study, the reduced transition matrix element for the T(A,X)R transfer reaction is given on the basis of the distorted wave Born approximation method corresponding to a one-step direct transfer process [10]

$$T^{ll'} = \int d\vec{r}_{TC} \, . d\vec{r}_{XC} \quad \psi^{*(-)}_{XR}(\vec{K}_X, \vec{r}_{XR}) \quad \phi^{*l'j'}_{TC}(\vec{r}_{TC}) . \\ V_{XC}(\vec{r}_{XC}) \quad \phi^{lj}_{XC}(\vec{r}_{XC}) \; \psi^{(+)}_{AT}(\vec{K}_A, \vec{r}_{AT}) \qquad (1)$$

where ψ's and ϕ's are respective distorted- and bound state-wave functions. In order to obtain an explicit analytic expression for the reduced transition element, the interaction potential between the particles T and X is assumed to be [11] not too different from the one between the particles X and R ($V_{TX} \approx \widetilde{V}_{XR}$). For this case, the distorted wave functions $\psi^{(+)}$ and $\psi^{(-)}$ as being functions of composed variables $\vec{r}_{AT}$ and $\vec{r}_{XR}$ can be expanded by Taylor expansion. Then, we get for the reduced form factor $F(r)$ the expression as

$$F(r) = \int d\vec{r}_{XC} \quad e^{i\vec{r}_{XC}\cdot\vec{Q}} \, V_{XC}(\vec{r}_{XC}) \; \phi^{lj}_{XC}(\vec{r}_{XC}) . \qquad (2)$$

The function $e^{i\vec{r}_{XC}\cdot\vec{Q}}$ has been expanded in terms of the plane wave expansion

$$e^{i\vec{r}_{ij}\cdot\vec{Q}} = \sum_{l=0}^{\infty} (2l+1) \, i^l \; j_l(Qr_{ij}) \; p_l(\cos\theta) \; , \qquad (3)$$

where $j_l(Qr_{ij})$ is the spherical Bessel function. In this analysis, the

bound-state interaction V_{XC} (r_{XC}) is taken to have Yukawa potential [12]. Then, the reduced form factor has the form

$$F(r) = V_{xc}^{0}\, N(l,....)\,(2l+1)\, e^{\frac{R_x+R_c}{a}} \int \frac{1}{(Z^2+Q^2)^2}\,.$$
$$.\left[\frac{Z}{2a}+\frac{1}{\sqrt{\pi}}\left(1-\frac{R_x+R_c}{2a}\right)\left(Z^2+Q^2\right)\right]\psi_{AT}^{(+)}(\vec{K}_A,\vec{r}_{TC})\,.$$
$$.\,\psi_{XR}^{*(-)}(\vec{K}_X,\frac{-M_A}{M_R}\vec{r}_{TC})\;\phi_{TC}^{*l'j'}(\vec{r}_{TC})\,d\,\vec{r}_{TC} \qquad (4)$$

The quantities which appeared are parameters of the bound-state form factor [12] based on the finite-range calculations [13]. In these calculations, the partial wave expansion is used for the distorted waves. For simplicity, we take the axis of quantization along $\vec{k}_A$ direction and the y-axis along the normal to the reaction plane $\vec{k}_A$ x $\vec{k}_x$.

NUMERICAL CALCULATIONS AND RESULTS

In the present section, only on outline of the technique needed in the DWBA calculations had been introduced to avoid needless repetition. The details of calculations are given explicitly following the finite-range effect [13]. In this analysis, the differential cross-sections as well as the form factors have been numerically calculated for the ^{48}Ca(^{16}O,^{14}C)^{50}Ti, ^{64}Ni(^{16}O,^{14}C)^{66}Zn, ^{16}O(^{7}Li,α)^{19}F and ^{24}Mg(^{16}O,^{12}C)^{28}Si reactions at different incident energies leaving the residual nuclei in different excited states. In a first set of calculations, the standard six-parameters Woods-Saxon optical potential [3] together with the Coulomb potential have been used to generate the initial and final distorted waves. The parameters of the optical potential are taken as those used in earlier calculations. These parameters (set I) are found to reproduce the forward angle data reasonably well but they don't fit the large angle data. Therefore, the starting potential parameters are varied to obtain the best fit to the data by minimizing χ^2. The resulting parameters (set II) are given in Table 1. The results obtained for the differential cross-sections are shown in figures (2)- (5) by the dashed lines together with previous calculations shown by the dotted lines. As shown in figure (1), the form factors behave in a typical behavior shapes for all considered reactions. Therefore, we are left with the (^{16}O,^{14}C) form factor as the standard in the present calculations. Generally, it is found that the fits to

the data are quite good over the entire angular range as shown in figures (2) and (3) but the predictions are too low in magnitude at large angles as seen in figures (4) and (5). In fact, different values of the normalization factors have been used. The best fit to the experimental data was achieved, with factors given in Table 2.

Table (1): Optical potential parameters used in the DWBA calculations

Channel	Set	V_0 (MeV)	r_v (fm)	a_v (fm)	W_0 (MeV)	R_w (fm)	a_w (fm)	r_c (fm)
$^{14}C + {}^{50}Ti$	I	33.90	1.344	0.424	110.2	1.274	0.280	1.3
$^{14}C + {}^{66}Zn$	I	35.90	1.35	0.43	101.5	1.274	0.28	1.25
	II	33.79	1.25	0.58	19.11	1.284	0.48	1.25
$^{16}O + {}^{48}Ca$	I	33.90	1.344	0.424	110.2	1.274	0.28	1.3
	II	100.1	1.207	0.50	24.0	1.207	0.482	1.2
$^{16}O + {}^{64}Ni$	I	70.0	1.207	0.57	106.0	1.207	0.39	1.25
	II	45.0	1.207	0.69	20.0	1.207	0.69	1.25
$^{16}O + {}^{24}Mg$	I	37.0	1.37	0.39	78.0	1.32	0.20	1.2
$^{12}C + {}^{28}Si$	I	37.0	1.37	0.39	78.0	1.32	0.20	1.3
	II	13.7	1.39	0.40	62.0	0.93	0.43	1.2
$^{7}Li + {}^{16}O$	I	240.6	1.19	0.73	16.3	2.08	0.71	1.20
	II	100.4	1.30	0.81	45.0	1.26	1.16	1.30
	III	189.5	1.21	0.74	21.3	2.00	0.82	1.30
$^{4}He + {}^{19}F$	I	180.0	1.42	0.56	16.5	1.42	0.56	1.40
	II	170.0	1.21	0.77	11.38	2.10	0.95	1.30

$$f(r_i) = \left\{1 + \exp[(r - R_i)/a_i]\right\}^{-1}$$

$$R_i = r_o\left(A_1^{1/3} + A_2^{1/3}\right) \qquad \text{for } i = \text{v, w and c}$$

$r_o = r_c = 1.25$ fm and $\Delta = 0.80$ fm

Table (2): Bound-state Parameters

State	E (MeV)	r_o[a] (fm)	a (fm)
$^{7}L_i = {}^{4}He \oplus t\ (0^+\ g.s.;2p)$	2.46	1.26	0.65
$^{16}O = {}^{12}C \oplus {}^{4}He\ \ (0^+\ g.s.;2s)$	7.16	1.20	0.60
$^{19}F = {}^{16}O + t\ (\ (1/2)^-, (3/2)^-, (5/2)^-\ ;\ 4p\text{-}1h)$	b	1.26	0.65

a) $R_{bound} = r_o \left(A_1^{1/3} + A_2^{1/3}\right)$ fm

b) Adjust to give a binding energy of 11.699 MeV - E_{exc}

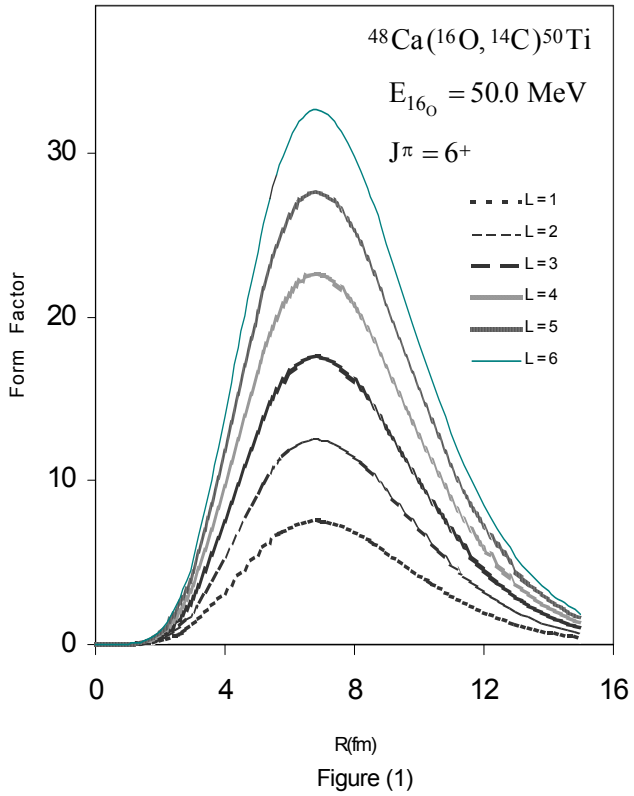

Figure (1)

Figure (1): Yukawa form factors of $^{48}Ca(^{16}O, ^{14}C)^{50}Ti$ reaction for different angular momenta with Woods-Saxon form factors potential parameters (set II).

Figure (2): The angular distributions of the $^{48}Ca(^{16}O, ^{14}C)^{50}Ti$ two-nucleon transfer reaction at 50.5 MeV incident energy leading to 0.0 and 3.20 MeV different ^{50}Ti excited.
The solid lines (—) are the present DWBA calculations using (WS+JD) potential.
The dashed lines (- - -) are the present DWBA calculations using (WS+WS) potential.
The dots (•) are the experimental data taken from reference [15].

Figure (3): The angular distributions of the ^{64}Ni(^{16}O, ^{14}C)^{66}Zn two-nucleon transfer reaction at 56.0 MeV incident energy leading to 0.0, 1.04 and 2.83 MeV different ^{66}Zn excited states.
The solid lines (—) are the present DWBA calculations using (WS+JD) potential.
The dashed lines (- - -) are the present DWBA calculations using (WS+WS) potential.
The dots (•) are the experimental data taken from reference [15].

Figure (4): Differential cross-sections of the $^{16}O(^{6}Li, \alpha)^{18}F$ three-nucleon transfer reaction at 20.0 MeV incident energy leading to 0.11, 1.35 and 1.46 MeV different ^{19}F excited states.
The solid lines (—) are the present DWBA calculations using (WS+JD) potential.
The dashed lines (- - -) are the present DWBA calculations using (WS+WS) potential.
The dots (•) are the experimental data taken from reference [16].

Figure (5): Differential cross-sections of the $^{24}Mg(^{16}O, ^{12}C)^{32}Si$ (g.s.) reaction at 35.5 MeV incident energy.
The solid lines (—) are the present DWBA calculations using (WS+JD) potential.
The dashed lines (- - -) are the present DWBA calculations using (WS+WS) potential.
The dots (•) are the experimental data taken from reference [17].

In a second set of analysis, the imaginary optical potential is demonstrated by the angular momentum- dependent potential [14]. The obtained results are introduced by solid curves in figures (2) – (5). It is found that calculations employing J-dependent absorptive potential yield

result comparable to those using real and imaginary Woods-Saxon potential at forward angles. This is because, the inclusion of the J-dependent term improves the cross-sections magnitude and leads to reasonable results better than Woods-Saxon potential at large angles. Additionally, the oscillatory structures of the calculated differential cross-sections at the forward angles are found to change appreciably with the choice of the optical model potentials. In these calculations, the bound-state wave functions are constructed by the usual Woods-Saxon potential with radius r_o= 1.25fm and diffuseness a = 0.65 fm. Where the potential depth is adjusted to reproduce the particle- particle separation energies. The number of nodes N of the radial wave functions was calculated from the harmonic oscillator relation. By matching the present DWBA calculations of the differential cross-sections with the experimental data, the spectroscopic factors in each reaction state are extracted as

$$\frac{\left(d\sigma/d\Omega\right)_{\text{exp.}}}{\left(d\sigma/d\Omega\right)_{theor.}} = \text{N} \cdot \frac{C^2}{(2J+1)} \cdot \text{S}_{ij} \ , \qquad (5)$$

where N is the normalization factor and C^2 stands for isospin factor. The obtained values of these factors are listed in Table 3.

Table (3): Spectroscopic Factors

Reaction	Incident energy (MeV)	Excitation energy (MeV)	J^π	Previous	Present Spectroscopic factors (WS+WS)	Present Spectroscopic factors (WD+JD)	N $Mev^2.fm^3$
$^{48}Ca\ (^{16}O, ^{14}C)\ ^{50}Ti$	50.5	0.00	0^+	0.67	0.81	0.89	$15x10^4$
		3.20	6^+	0.66	0.84	0.87	
$^{64}Ni\ (^{16}O, ^{14}C)\ ^{66}Zn$	56.0	0.00	0^+	0.62	0.76	0.76	
		1.04	2^+	0.61	0.74	0.73	
		2.83	3^-	0.62	0.78	0.76	
$^{16}O\ (^{7}Li, \alpha)\ ^{19}F$	20.0	0.110	$\frac{1}{2}^+$	0.35	0.66	0.71	$20x10^4$
		1.35	$\frac{5}{2}^-$	0.40	0.64	0.71	
		1.46	$\frac{3}{2}^-$	0.59	0.65	0.73	
$^{24}Mg\ (^{16}O, ^{12}C)\ ^{28}Si$	35.5	0.00	0^+		0.76	0.83	$15x10^4$

DISCUSSION AND CONCLUSIONS

In the present work, different heavy-ion transfer reactions have been studied within the framework of the DWBA calculations using optical potential model. The calculated angular distributions using both of (WS+WS) and (WS+JD) are found to be in a good agreement with the experimental data in the forward angle region. In general, although the calculated forward cross-sections are found to be equivalent and close enough in such cases but the inclusion of the J-dependent term introduces a substantially better description of the large angle data than Woods-Saxon potentials. Therefore, the present analysis exhibits the important contributions of the J-dependant absorptive term to account for the phase and amplitude of the angular distributions as well as the magnitude of the cross-sections at large angular range.

In conclusion, we conclude that the present one-step DWBA calculations reproduce the magnitude and shape of the experimental differential cross-sections reasonably well in both forward- and large-angle regions.

REFERENCES

1. Y. Sugiyama, Y, Tomita, H.Ikezoe, K.Ideno, N.Shikazono, N.Kato, H.Fujita, T.Sugimitsu and S.Kubono, *Phys.Lett*., **1986,** B176, 302.
2. F.Videbaek, Ole Hansen, B.S.Nilsson, E.R.Flynn and J.C.Peng, *Nucl. Phys*., **1985,** A433, 441.
3. Y. Kondo and T. Tamura, *Phys. Rev*., **1984,** C30, 97.
4. C.-Q.Gao, P.–Z.Ning and G.–Z.He, *Nucl. Phys*., **1988**, A485, 282.
5. L.–H.Xia and G.–Z.He, *Nucl. Phys*., **1988**, A485, 291.
6. R.Lichtenthaler Filho,A.Le/pine- Szily,A.C.C.Villari and O.P.Filho, *Phys. Rev*., **1989**, C39, 884.
7. A.Kabir, M.W.Kermod and N.Rowley, *Nucl. Phys*., **1988**, A481, 94.
8. S.K.Charagi, S.K.Gupta, M.G.Betigeri, C.V.Fernandes and Kauldeep, *Phys. Rev*., **1993**, C48, 1153.
9. D.E.Treka, A.D.Frawley, K.W.Kemper, D.Robson, J.D.Fex and E.G.Myers, *Phys. Rev*., **1990**, C41, 2134.
10. G.R.Satcler, *Nucl. Phys*., **1964**, 55, 1.
11. T. Tamaura, *Phys. Reports* **1974,** 14(2), 59.

12. B.Sikora, M.Blann, W.Bisphinghoff and Beckerman, *Phys. Rev*. **1980**, C21, 614.
13. A.Osman and A.A.Farra, *IL Nuovo Cimento* ,**1990**, A103, 1693.
14. Y.Kondo, B.A.Robson, R.Smith and H.H.Wolter, *Phys. Lett*., **1985**, B162, 39.
15. M.C.Mermaz, *Phys. Rev*.,**1980**, C21, 2356.
16. S.Mordechai and H.T.Fortune, *Phys. Rev*.,**1984**, C30, 1924.
17. S.J.Sanders, H.Ernst, W.Henning, C.Jachcinsk, D.G.Kovar, J.P.Schiffer and J.Barrette, *Phys. Rev*., **1985**, C31, 1775.